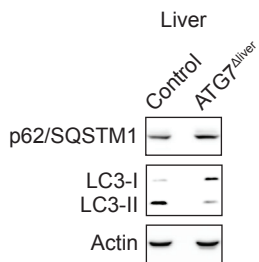
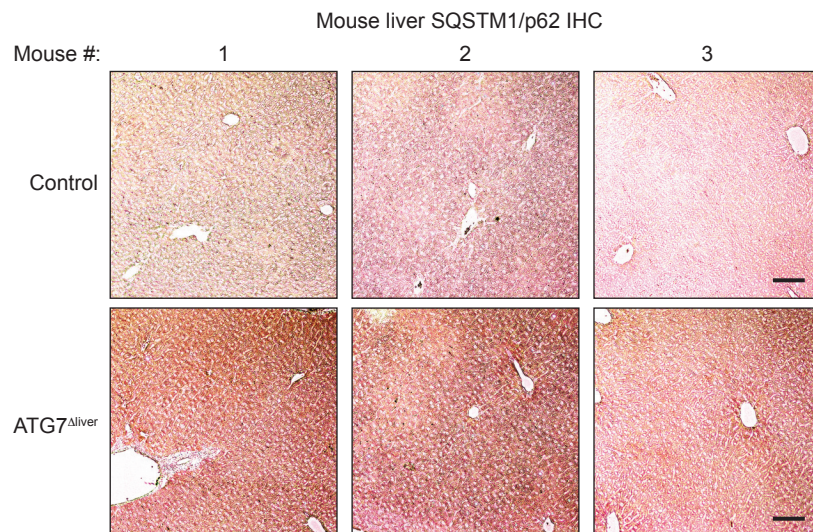
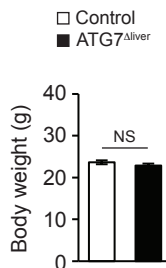


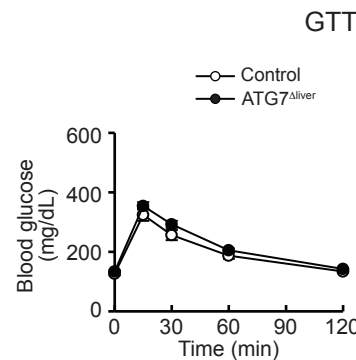
Fig. S1

A**B****C**

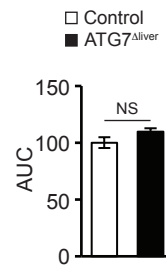
RD



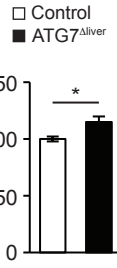
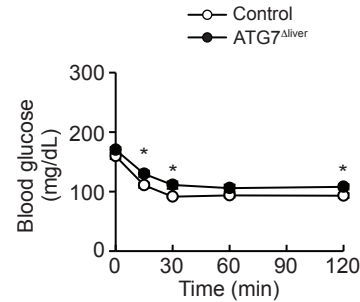
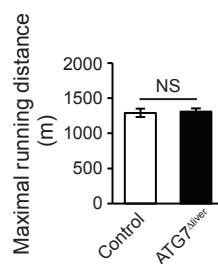
D



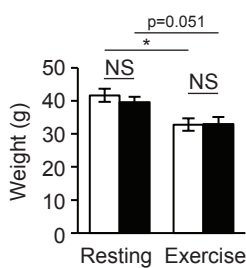
RD



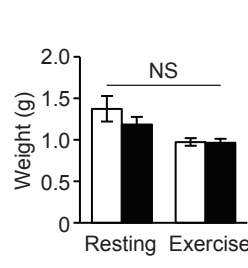
ITT

**E****F**

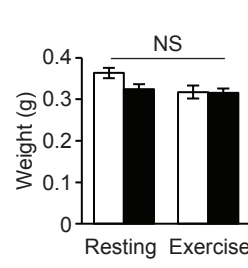
Body weight



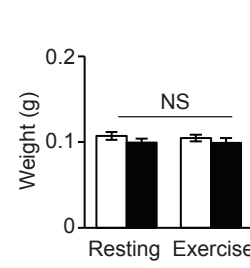
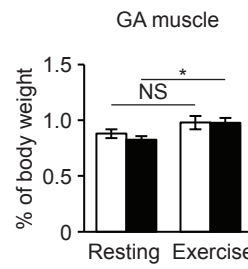
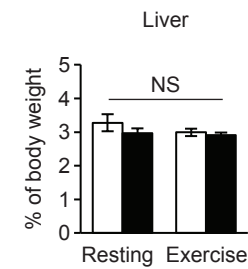
Liver



GA muscle



TA muscle

□ Control
■ $\text{ATG7}^{\Delta\text{liver}}$ 

TA muscle

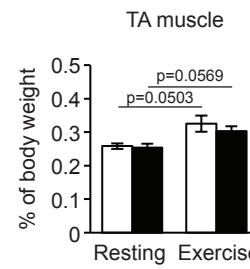
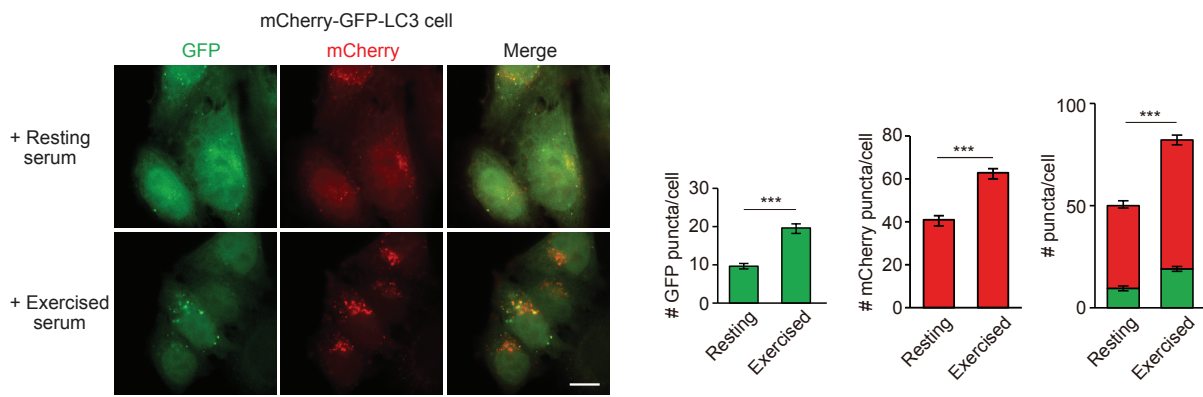


Figure S1. Autophagy markers, body weight, glucose tolerance and insulin tolerance of control and ATG7^{Δliver} mice under regular diet (RD) feeding, and their maximal exercise capacity and endpoint tissue weight after concurrent HFD and exercise treatment, related to Figure 1.

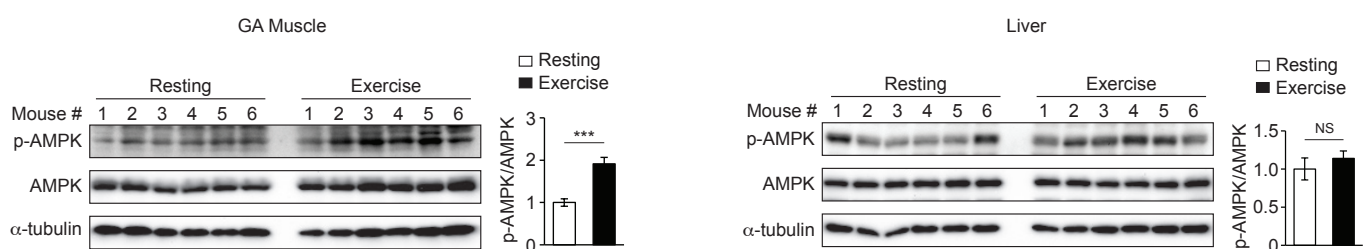
(A) WB analysis of p62/SQSTM1, non-lipidated LC3-I and lipidated LC3-II in the liver of control and ATG7^{Δliver} mice. (B) Immunohistochemistry (IHC) staining of p62/SQSTM1 in the liver of 3 control and 3 ATG7^{Δliver} mice. Bar, 100 µm. (C-D) Comparable body weight (C), GTT and ITT (D) of control and ATG7^{Δliver} mice fed with RD. Control mice, N=12; ATG7^{Δliver} mice, N=21. (E-F) Maximal running distance (E), and exact and relative weight of skeletal muscle and liver (F) of control and ATG7^{Δliver} mice analyzed at the end of the study (HFD feeding with or without daily 50-min exercise for 10 weeks). GA, gastrocnemius; TA, tibialis anterior. (E) N=6-9; (F) N=6-12. (C-E), t-test. (F), one-way ANOVA with Tukey-Kramer test. *, P<0.05; NS, not significant.

Fig. S2

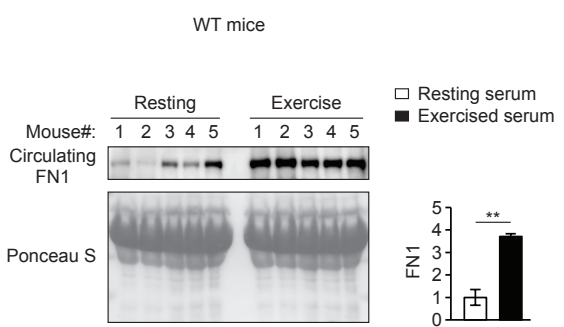
A



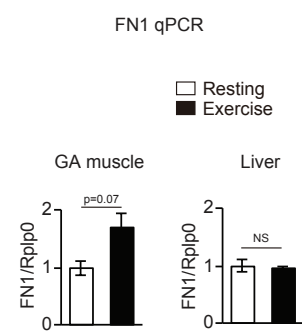
B



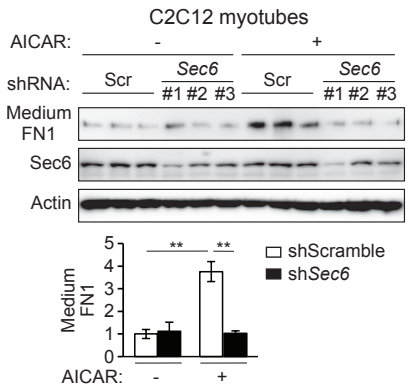
C



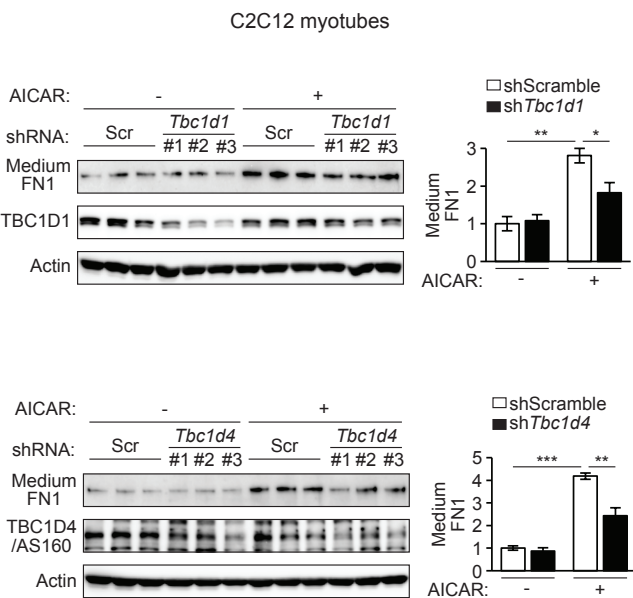
D



E



F



G

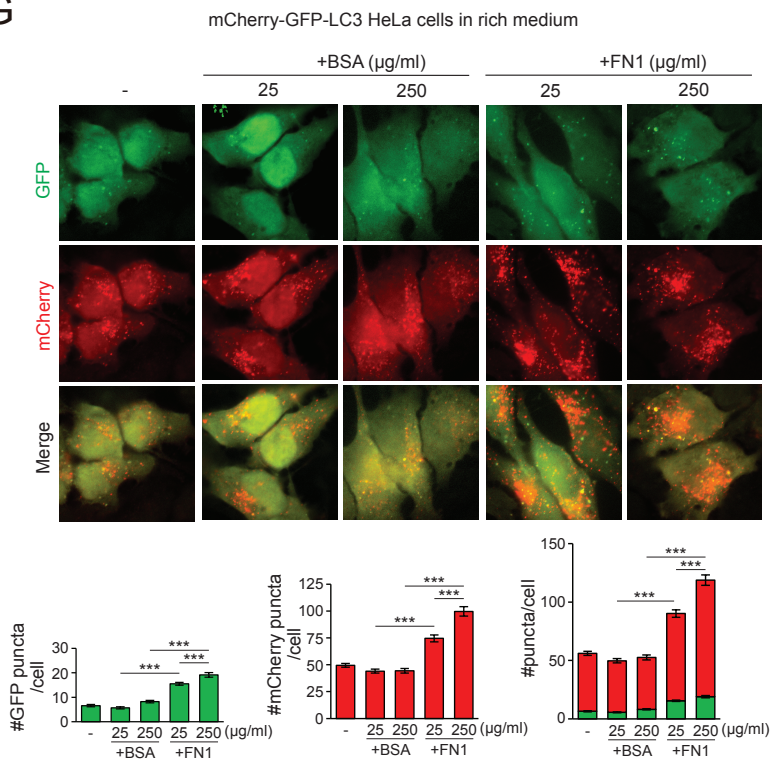


Figure S2. Exercise induces FN1 secretion, which activates autophagy, related to Figure 2.

(A) Representative images and quantification of autolysosomes (red) and autophagosomes (green) in HeLa cells stably expressing tandem mCherry-GFP-LC3 cultured for 3 h in medium containing 10% serum from WT mice at rest or after 90-min treadmill running. Bar, 15 μ m. 70-80 cells per mouse were analyzed. **(B)** WB analyses and quantification of AMPK phosphorylation levels in the gastrocnemius (GA) muscle and liver of WT mice at rest or after 90-min exercise. N=6. **(C)** WB of serum FN1 in WT mice at rest or after 90-min exercise. N=5. **(D)** qPCR of FN1 in the GA muscle and liver of WT mice at rest or after 90-min exercise. N=6. **(E-F)** The exocyst component Sec6 **(E)**, and **(F)** two closely related RabGAPs TBC1D1 and TBC1D4/AS160, regulate AICAR-induced FN1 secretion from myotubes. WB of FN1 in the conditioned medium of C2C12-differentiated myotubes stably expressing scrambled (Scr), Sec6 **(E)**, Tbc1d1 or Tbc1d4 **(F)** shRNAs treated with vehicle or 1 mM AICAR for 1 h. Briefly, on day 5 of myotube differentiation, shRNAs were delivered into the C2C12 cells via lentivirus to induce gene knockdown, and medium FN1 was measured on day 9. N=3. **(G)** Representative images and quantification of autolysosomes (red) and autophagosomes (green) in mCherry-GFP-LC3 HeLa reporter cells cultured in nutrient-rich medium containing two different concentrations of FN1 or BSA for 3 h. N=50 cells. **(A-D)**, t-test. **(E-G)**, one-way ANOVA with Tukey-Kramer test. *, P<0.05; **, P<0.01; ***, P<0.001; NS, not significant.

Fig. S3

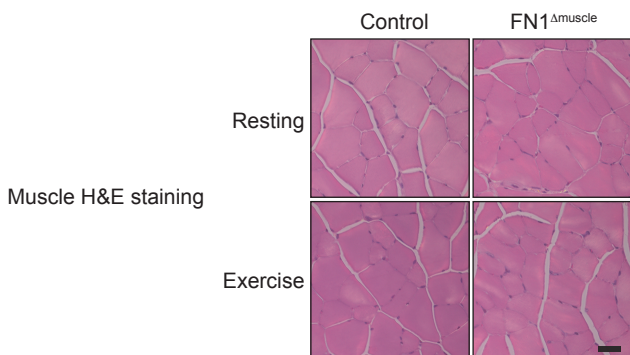
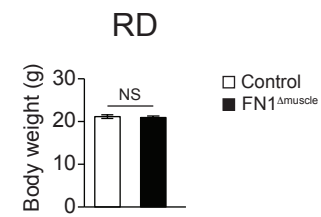
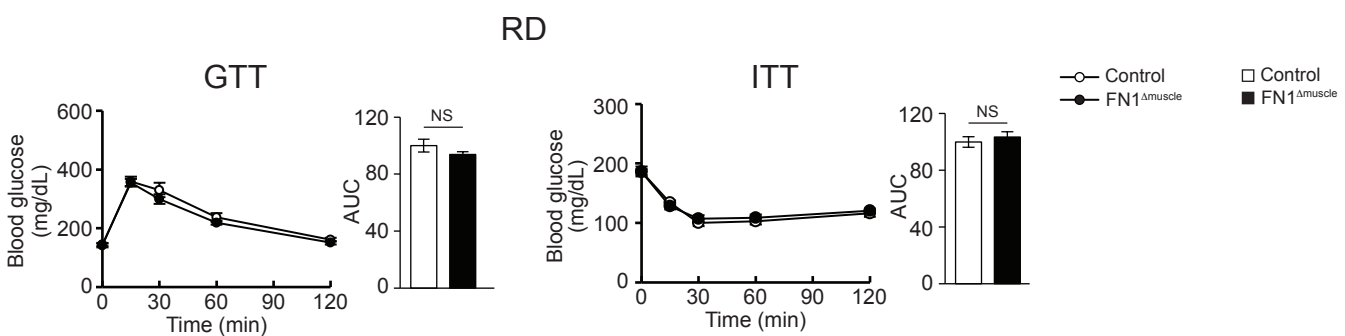
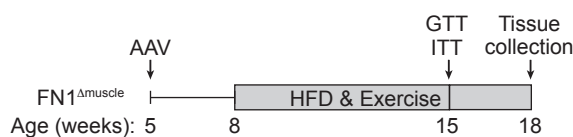
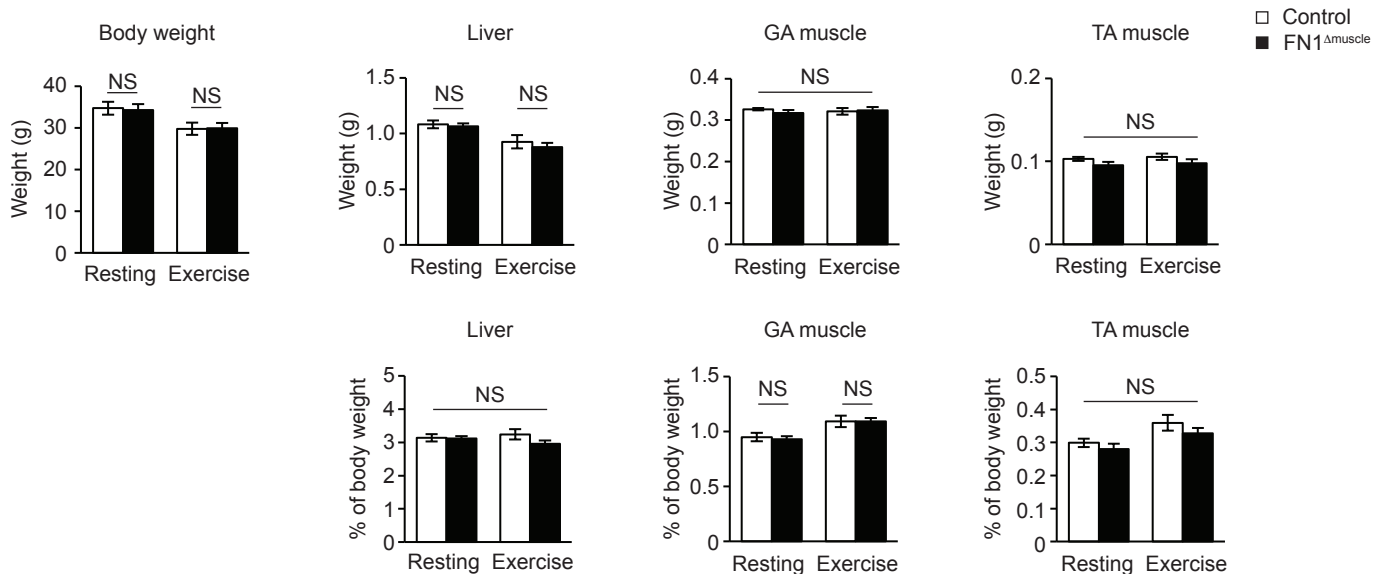
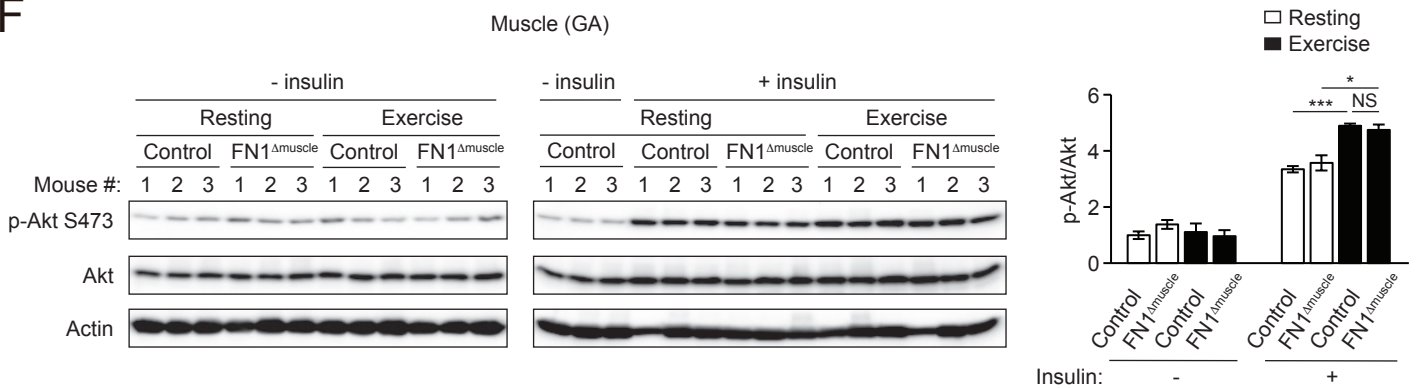
A**B****C****D****E****F**

Figure S3. Muscle-specific depletion of FN1 does not affect muscle morphology, body weight, glucose tolerance and insulin tolerance under RD feeding, or exercise-induced insulin sensitization in muscle and endpoint tissue weight after concurrent HFD and exercise treatment, related to Figure 3.

(A) H&E staining of skeletal muscle of control and $\text{FN1}^{\Delta\text{muscle}}$ mice at rest or after 90-min exercise. Bar, 25 μm . **(B-C)** Comparable body weight **(B)**, GTT and ITT **(C)** of control and $\text{FN1}^{\Delta\text{muscle}}$ mice fed with RD. N=14-16. **(D)** Experimental design of HFD feeding and exercise training in control and $\text{FN1}^{\Delta\text{muscle}}$ mice. **(E)** Exact and relative weight of skeletal muscle and liver of control and $\text{FN1}^{\Delta\text{muscle}}$ mice analyzed at the end of the study (HFD feeding with or without daily 50-min exercise for 10 weeks). GA, gastrocnemius; TA, tibialis anterior. N=6-9. **(F)** Insulin-stimulated Akt phosphorylation in the GA muscle of control and $\text{FN1}^{\Delta\text{muscle}}$ mice fed with HFD with or without daily 50-min exercise for 7 weeks, and then injected with 2 U/kg insulin 15 min prior to tissue collection. The “- insulin resting” controls were loaded twice on both gels to allow for normalization of samples to the same controls. N=3. **(B-C)**, t-test. **(E-F)**, one-way ANOVA with Tukey-Kramer test. *, P<0.05; ***, P<0.001; NS, not significant.

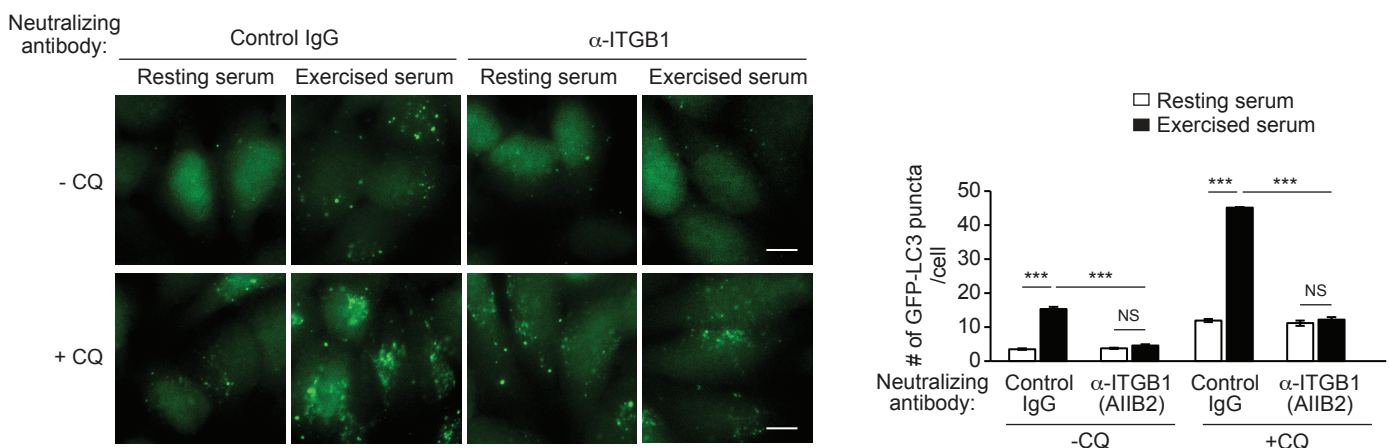
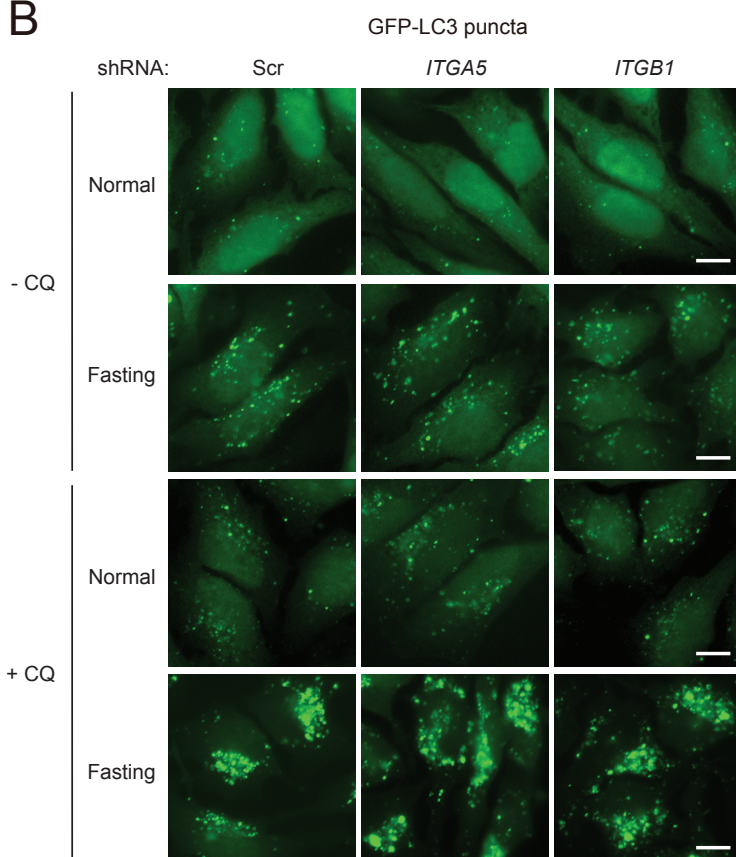
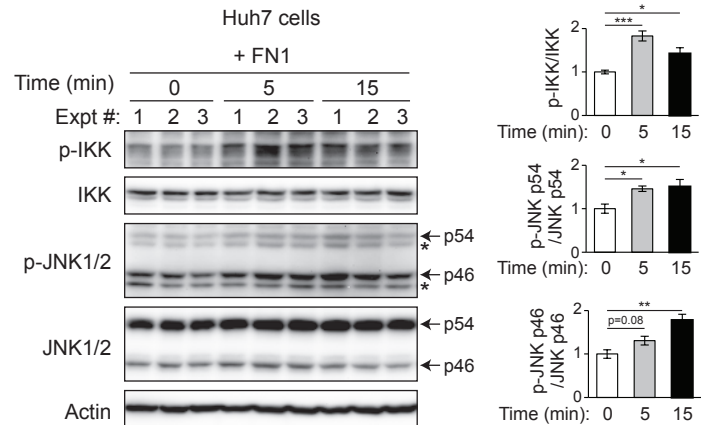
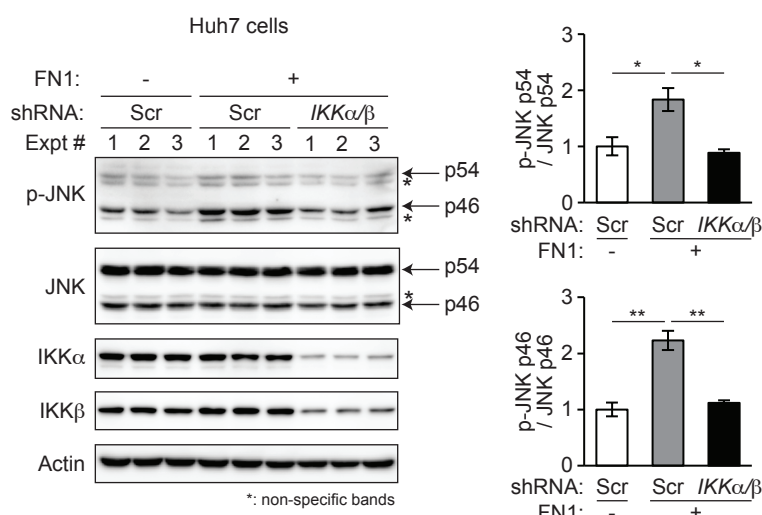
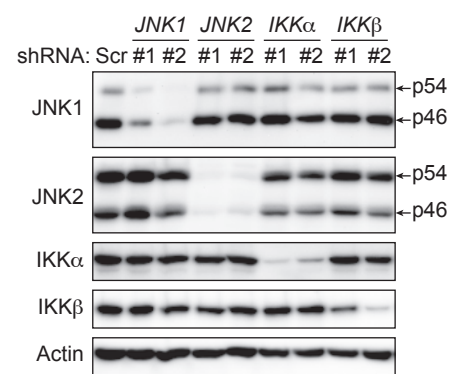
A**B****C****D****E**

Figure S4. Characterization of an autophagy-inducing $\alpha 5\beta 1$ integrin-IKK-JNK pathway, related to Figure 4.

(A) Representative images and quantification of GFP-LC3 puncta in GFP-LC3 HeLa cells cultured for 3 h in medium containing 10% serum from WT mice at rest or after 90-min treadmill running and 20 μ g/ml ITGB1 antibody or control IgG, with or without chloroquine (CQ, 10 μ M). Bar, 10 μ m. N=3 mice. 50 cells per mouse were analyzed. One-way ANOVA with Tukey-Kramer test. (B) $\alpha 5\beta 1$ integrin is not required for basal or fasting-induced autophagy. Representative images of GFP-LC3 puncta in GFP-LC3 HeLa cells expressing scrambled (Scr), ITGA5 or ITGB1 shRNA cultured in normal or fasting (EBSS) medium in the presence or absence of the lysosomal inhibitor chloroquine (CQ) for 3 h. Bar, 10 μ m. (C) WB analysis of IKK and JNK1/2 phosphorylation in Huh7 hepatic cells treated with 100 μ g/ml FN1 for the indicated time course. *, non-specific band. N=3. One-way ANOVA with Dunnett's test. (D) Huh7 cells stably expressing Tet-inducible scrambled (Scr) shRNA, or both IKK α and IKK β shRNAs, were treated with Tet for 72 h and then with 100 μ g/ml FN1 for 5 min. Levels of JNK phosphorylation were analyzed by WB. N=3. One-way ANOVA with Tukey-Kramer test. (E) WB analysis of gene knockdown efficiency in GFP-LC3 HeLa cells stably expressing Tet-inducible scrambled (Scr), IKK α , IKK β , JNK1 or JNK2 shRNA treated with Tet (1 μ g/ml) for 72 h. *, P<0.05; **, P<0.01; ***, P<0.001; NS, not significant.

Fig. S5

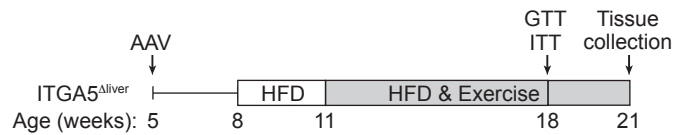
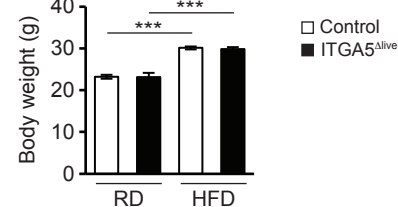
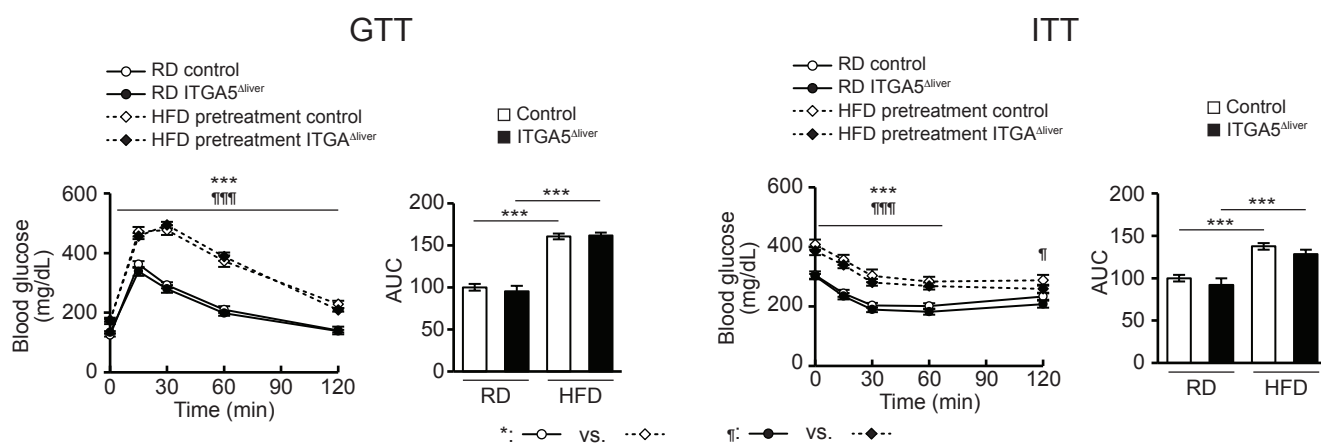
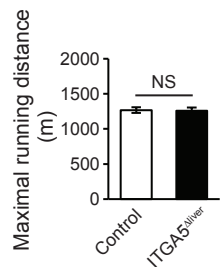
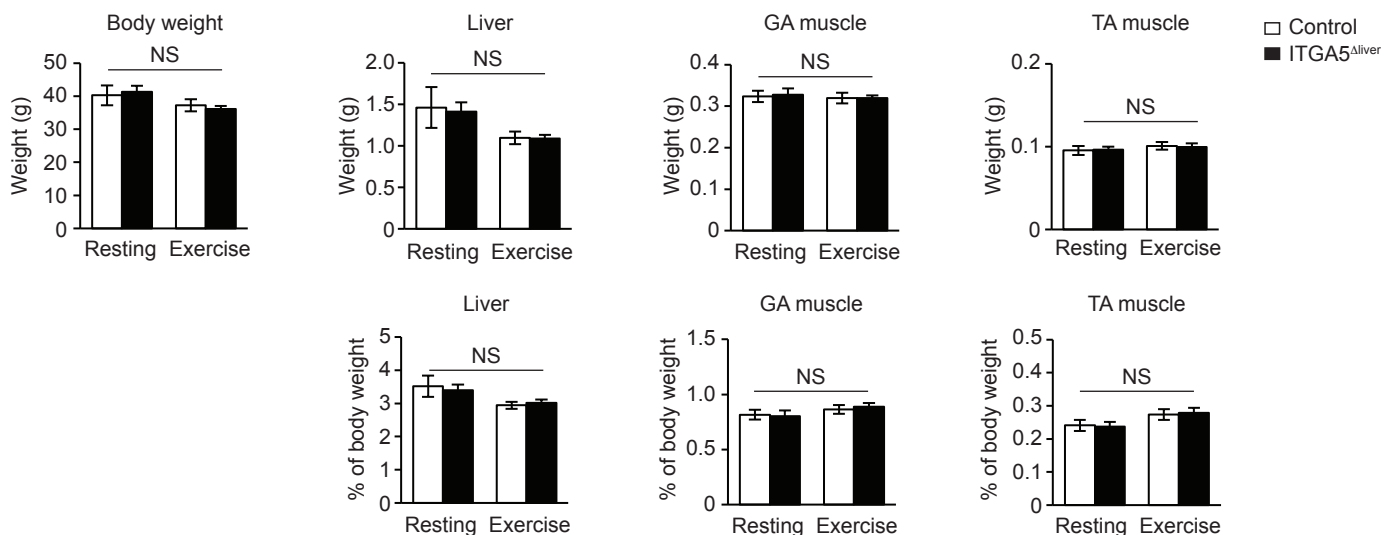
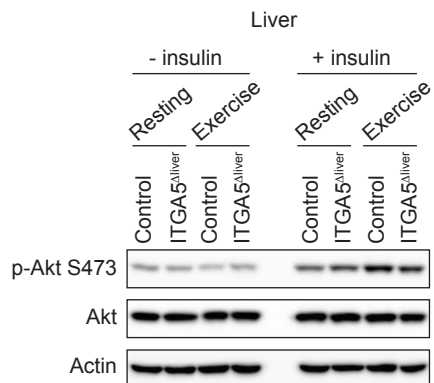
A**B****C****D****E****F**

Figure S5. Liver-specific depletion of $\alpha 5$ integrin does not affect body weight, glucose tolerance and insulin tolerance under RD or HFD feeding without exercise, or maximal exercise capacity and endpoint tissue weight after concurrent HFD and exercise treatment, related to Figure 5.

(A) Experimental design of HFD feeding and exercise training in control and ITGA5 $^{\Delta liver}$ mice. (B-C) Comparable body weight (B), GTT and ITT (C) of control and ITGA5 $^{\Delta liver}$ mice fed with RD or 3-week HFD with no exercise. N=12-18. (D-E) Maximal running distance (D), and exact and relative weight of skeletal muscle and liver (E) of control and ITGA5 $^{\Delta liver}$ mice analyzed at the end of the study (HFD feeding with or without daily 50-min exercise for 10 weeks). GA, gastrocnemius; TA, tibialis anterior. N=6-9. (F) Representative WB image of insulin-stimulated Akt phosphorylation in the liver of control and ITGA5 $^{\Delta liver}$ mice fed with HFD with or without daily exercise for 7 weeks, and then injected with 2 U/kg insulin 15 min prior to tissue collection. (B-C, E), one-way ANOVA with Tukey-Kramer test. (D), t-test. ***, ¶¶¶, P<0.001; NS, not significant.

Table S1. shRNA target sequences. Related to the STAR METHODS section.

Target gene	#	shRNA target sequences	Virus type
Mouse <i>Fn1</i>	1	5'-GCCTAGAAATACCTTCTCTTA-3'	AAV
Mouse <i>Itga5</i>	1	5'-AGACCTCTTGAGCGGGAATA-3'	
Mouse <i>Atg7</i>	1	5'-AAAGTTCTTGATCAGTACGAGC-3'	
Human <i>ITGA5</i>	1	5'-CTCCTATATGTGACCAGAGTT-3'	
	2	5'-CTCAGGCCAGCCCTACATTAT-3'	
Human <i>ITGB1</i>	1	5'-GCCTTGCATTACTGCTGATAT-3'	
	2	5'-TAGGTAGCTTAGGGCAATAT-3'	
Human <i>JNK1</i>	1	5'-GCCAGTAATATAGTAGTAAA-3'	Lentivirus
	2	5'-GCAAATCTTGCCAAGTGATT-3'	
Human <i>JNK2</i>	1	5'-CTAACTTATGTCAGGTTATT-3'	
	2	5'-GCTTCTGAAGTTATCTCTTAA-3'	
Human <i>IKKα</i>	1	5'-GCAGATGACGTATGGGATATC-3'	
	2	5'-GCAAATGAGGAACAGGGCAAT-3'	
Human <i>IKKβ</i>	1	5'-CCAGCCAAGAAGAGTGAAGAA-3'	
	2	5'-CGGAAGTACCTGAACCAGTTT-3'	
Mouse <i>Sec6</i>	1	5'-GCTGTCATGCAGAACCGTATT-3'	
	2	5'-CCCACACTGTTATGTGCAGTA-3'	
	3	5'-CCTCTGACATGGTCCTAAA-3'	
Mouse <i>Tbc1d4</i>	1	5'-CATGTCAGAACGGAGATCTTAA-3'	
	2	5'-AGTGCCAAGACGCAGATTAAA-3'	
	3	5'-TTCTAGGAAGTGCTGATTATT-3'	
Mouse <i>Tbc1d1</i>	1	5'-CCGAGCAGATATGAAGATTAT-3'	
	2	5'-TATCGGCCAGACATGATTATT-3'	
	3	5'-GAAGAGACTGTGCA CCATTAA-3'	

Table S2. Primer sequences for qPCR. Related to the STAR METHODS section.

Target gene	Forward primer (5'→3')	Reverse primer (5'→3')
Mouse <i>Rplp0</i>	TTCGTGTTCACCAAGGAGGAC	ATGATCAGCCCAGAGGAGAAG
Mouse <i>Fn1</i>	ATCGCATTGGGATCAGTGG	CACTGGTCAATGGGTCACAC